

Cyclodextrin-Confined Supramolecular Lanthanide Photoswitch

Hua-Jiang Yu, Haoran Wang, Fang-Fang Shen, Feng-Qing Li, Ying-Ming Zhang,*
Xiufang Xu, and Yu Liu*

The utilization of azobenzene-based photoisomerization cannot only control the morphology of supramolecular assemblies, but can also regulate many biological processes. However, the design of azobenzene-involved nanoconstructs with switchable photoluminescence remains challenging because of the light-quenching ability of azobenzene. Herein, an azobenzene-derived multicomponent nanosystem is reported and its function as a supramolecular lanthanide photoswitch is explored. The metal chelation between lanthanide ions ($\text{Ln}^{3+} = \text{Eu}^{3+}$ and Tb^{3+}) and 2,6-pyridinedicarboxylic acid is utilized as the light-emitting center but its inherent fluorescence emission is completely suppressed via the disordered motion of the adjoining azophenyl unit. Interestingly, the hydrophobic cavity of α -cyclodextrin can provide a confined microenvironment to immobilize the molecular conformation of *trans*-azobenzene, thus leading to the recovery of characteristic lanthanide luminescence both in aqueous solution and the hydrogel state. Also, the luminescence can be reversibly turned off when the *cis*-azobenzene is expelled from the cavity of α -cyclodextrin upon alternating light irradiation. This mutual cooperation arising from host–guest complexation and metal–ligand coordination confers the desired photoswitchable luminescence abilities on the commonly used azobenzenes, which may hold great promise in the creation of more advanced light-responsive smart materials.

construct such materials is to incorporate functional sites into a multicomponent system that can precisely respond to the external stimuli.^[10–13] To this end, photochromic compounds, featuring the light-triggered reversible interconversion with distinct structural changes, have been frequently utilized as the building blocks to attain photo-responsive supramolecular assemblies.^[14–16] In particular, owing to the chemically modifiable molecular skeleton and high photoisomerization efficiency, azobenzene, and its derivatives have been viewed as excellent candidates to construct optically active nanoassemblies/devices with broad applications.^[17–20] More interestingly, azobenzene can form diverse supramolecular nanoconstructs with many cavity-bearing macrocycles through host–guest complexation.^[21–24] For instance, the *trans*-azobenzene can be tightly encapsulated into the cavity of cyclodextrins (CDs), whereas the bulky *cis*-isomer is prone to slide from the cavity. These large disparities in binding strengths highlight the promise of azobenzene as a general component to remotely control the aggregation

and disaggregation of cyclodextrin (CD)-based supramolecular assemblies using light.^[25–27]

Nevertheless, most of common azobenzenes are believed as non-fluorescent and even light-absorbing agent because the excited fluorophore can be deactivated by the ultrafast conformational change around the central N=N bond,^[28–30] which can greatly hinder their development in luminescent materials and biological imaging. To circumvent this limitation, several methods have been proposed to activate the luminescence of azobenzene derivatives, such as biochemical reduction of azo bond under hypoxia environment^[31] and coordination of N=N double-bond with heteroatoms.^[32,33] Unfortunately, the loss of reversible photochromism property inevitably occurs in these cases. Moreover, some uncommon azo-compounds,^[34] azobenzene-bridged cyclophane^[35] and light-driven molecular shuttles,^[36–37] have been created with tunable fluorescence emission, but simultaneously achieving high photoisomerization efficiency and distinct physicochemical outcomes remain a huge challenge. Even worse, the molecular sizes of over-engineered azo-compounds are not suitable for the host–guest complexation with native CDs. Therefore, it is essential to

1. Introduction

Recently, considerable endeavors have been dedicated to developing stimulus-responsive luminescent materials, due to their great potentials in biosensing/imaging,^[1–5] and multi-informational display.^[6–9] The conventional approach to

H.-J. Yu, H. Wang, F.-F. Shen, F.-Q. Li, Y.-M. Zhang, X. Xu, Y. Liu
College of Chemistry
State Key Laboratory of Elemento-Organic Chemistry
Collaborative Innovation Center of Chemical Science and Engineering
(Tianjin)
Nankai University
Tianjin 300071, P. R. China
E-mail: ymzhang@nankai.edu.cn; yuliu@nankai.edu.cn
Y. Liu
Haihe Laboratory of Sustainable Chemical Transformations
Tianjin 300192, P. R. China

 The ORCID identification number(s) for the author(s) of this article can be found under <https://doi.org/10.1002/sml.202201737>.

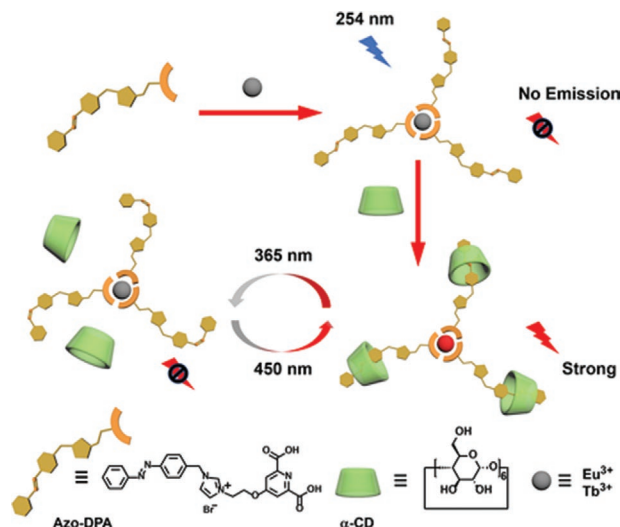
DOI: 10.1002/sml.202201737

develop a simple and feasible strategy to reversibly tune the photoluminescent behaviors of common azobenzenes.

Among the large variety of luminophores, lanthanide complexes stand out owing to their intriguing photophysical properties, including long-lived excited states, narrow and tunable emission bands, and large Stokes shifts.^[38–40] Although the combination of light-emitting lanthanide complexes with azobenzenes were sporadically reported in some known CD-based supramolecular nanosystems,^[41] no reversible photoluminescence has been achieved under such circumstance, to the best of knowledge. In this work, the introduction of lanthanide complex cannot only endow commonly used azobenzenes with desired photoluminescence activity but also offer an anchoring point for the tunable host–guest complexation with α -CD. As a result, strong lanthanide luminescence is recovered by the complexation with α -CD, because the nonradiative pathway of *trans*-azobenzene via molecular rotation is suppressed. Meanwhile, the luminescence is completely quenched when *cis*-azobenzene is escaped from the cavity of α -CD by alternating the irradiation wavelength. This CD-confined supramolecular lanthanide photoswitch can well work in both aqueous solution and hydrogel state, which will enrich the research content and advance the development of azobenzene-based photoluminescent supramolecular assemblies.

2. Results and Discussion

The construction of supramolecularly photoswitchable luminescent lanthanide complex ($\text{Ln}^{3+} = \text{Eu}^{3+}$ and Tb^{3+}) is depicted in **Scheme 1**. The synthetic routes of azobenzene-bearing pyridine-2,6-dicarboxylic acid (Azo-DPA) are shown in Chart S1 and Figures S1–S3 (Supporting Information). The introduction of imidazolium linker could greatly increase the water solubility of Azo-DPA. It is well-documented that azobenzenes can undergo reversible *trans*- and *cis*-photoisomerization upon light irradiation, and show strikingly distinct binding abilities toward α -CD. Therefore, ^1H NMR titration experiments were carried out to investigate the molecular binding behaviors of Azo-DPA with α -CD. As discerned from Figure S7 (Supporting Information), the azophenyl protons of *trans*-Azo-DPA exhibited a pronounced downfield shift upon stepwise addition of α -CD, while the protons of the pyridine-2,6-dicarboxylic acid remained almost unchanged. After validating the 1:1 binding stoichiometry by Job plot, the binding constant (K_S) was calculated to be $1.1 \times 10^4 \text{ M}^{-1}$ according to the nonlinear least-squares fitting method (Figure S8, Supporting Information). In addition, strong nuclear Overhauser effect (NOE) correlations were observed between the aromatic protons of azobenzene and the interior protons of α -CD in the rotating-frame Overhauser effect spectroscopy (ROSEY) spectrum (Figure S9a, Supporting Information). These results jointly demonstrate that the azophenyl unit of *trans*-Azo-DPA could be encapsulated in the cavity of α -CD to form a stable host–guest inclusion complex. In contrast, no obvious correlation peak was found after sufficiently exposed to UV irradiation, because the photoisomerized *cis*-azobenzene escaped from the α -CD's cavity (Figure S9b, Supporting Information). In addition, the chemical shifts of these characteristic protons returned to the original states



Scheme 1. Schematic illustration and molecular structures of $(\text{Ln}^{3+}@\text{Azo-DPA})\subset\alpha\text{-CD}$ complex as the cyclodextrin-confined supramolecular lanthanide photoswitch.

upon subsequent visible-light irradiation at 450 nm. By comparing the integral area of methylene protons adjacent to the azophenyl unit before and after light irradiation, it was found that although the conversion efficiency of *trans*-to-*cis* isomerization was kept at 71%, the degree of *cis*-to-*trans* isomerization increased from 67% to 78% with assistance of α -CD. This change is probably contributed to the high binding affinity between α -CD and *trans*-azobenzene, which can enrich the conformation of *trans*-isomer in solution and then facilitate the *cis*-to-*trans* conversion in the photochemical equilibrium reaction (**Figure 1a,b**).

To gain more insights into the photophysical properties, the photoisomerization process of Azo-DPA under light irradiation was further monitored by means of UV–vis absorption spectroscopy. As shown in Figure S10a (Supporting Information), the π – π^* transition absorption at 320 nm exhibited a significant decrease under the irradiation at 365 nm and the n – π^* transition absorption around 425 nm increased accordingly, indicating that *trans*-Azo-DPA was progressively converted into the *cis*-isomer with continuous UV light irradiation. Comparatively, the π – π^* absorption band was largely recovered upon the subsequent light irradiation at 450 nm, corresponding to the reverse isomerization from *cis* to *trans*-conformation. Similar spectroscopic behaviors were also observed in the case of $\text{Azo-DPA}\subset\alpha\text{-CD}$ complex and $(\text{Eu}^{3+}@\text{Azo-DPA})\subset\alpha\text{-CD}$ complex (**Figure 1c** and **Figure S11**, Supporting Information). According to the first-order kinetic equation, the rate constant for *trans*–*cis* photoisomerization was calculated to 0.0162 s^{-1} and this value increased to 0.0214 s^{-1} and 0.0206 s^{-1} for $\text{Azo-DPA}\subset\alpha\text{-CD}$ and $(\text{Eu}^{3+}@\text{Azo-DPA})\subset\alpha\text{-CD}$ complex, respectively (**Figure S12**, Supporting Information). Notably, the cycles could be completely repeated by five times at least without any fatigue (**Figure 1d**; **Figures S10b** and **S11b**, Supporting Information). Additionally, UV–vis absorption spectral changes of azo ligand and supramolecular complex were also investigated under continuous light irradiation at 254 nm. The π – π^* absorption band

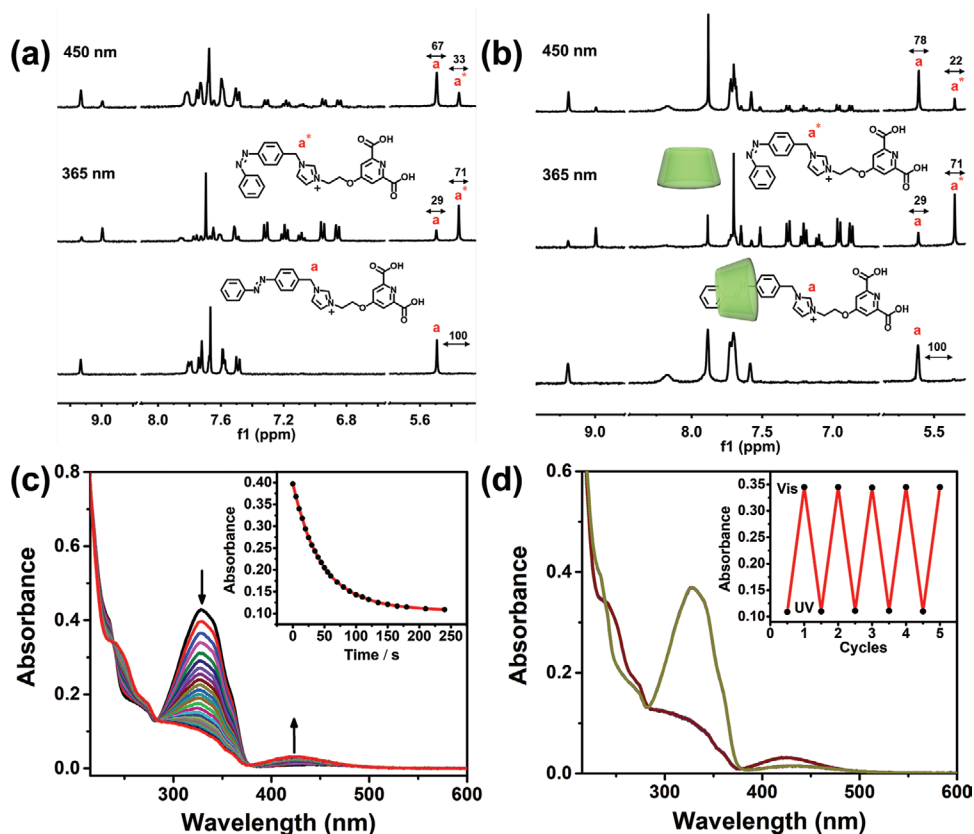


Figure 1. ^1H NMR spectra (400 MHz, D_2O , 298 K) of a) Azo-DPA (1.0×10^{-3} M) and b) Azo-DPA@ α -CD ($[\alpha\text{-CD}] = 3 \times 10^{-3}$ M) before and after UV light irradiation at 365 nm for 60 min, and subsequently exposed to visible-light irradiation at 450 nm for another 30 min. c) UV-vis spectral changes of Azo-DPA@ α -CD upon UV light irradiation at 365 nm and the corresponding absorbance changes at 320 nm (inset). d) UV-vis spectra of Azo-DPA@ α -CD upon alternating irradiation with UV (365 nm, 5 min) and visible light (450 nm, 40 s) in aqueous solution and the corresponding absorbance changes at 320 nm (inset) ($[\text{Azo-DPA}] = 0.02 \times 10^{-3}$ M, $[\alpha\text{-CD}] = 1 \times 10^{-3}$ M).

exhibited a decrease by $\approx 10\%$ and the photostationary state could be reached in 12 min under light irradiation at 254 nm (Figure S13, Supporting Information). Nevertheless, no obvious *trans*-to-*cis* photoisomerization could occur using 254 nm as the excitation wavelength, which would ensure the conformational fixation of azobenzene in the spectroscopic titration experiments.

Subsequently, the coordination interaction between Eu^{3+} and Azo-DPA was investigated. As shown in Figure S14 (Supporting Information), the optical transmittance of Azo-DPA rapidly decreased at 550 nm and reached the minimum in the presence of 1/3 equiv of Eu^{3+} , accompanied by the faint turbidity in solution. These phenomena were consistent with the 3:1 coordination stoichiometry between Azo-DPA and Eu^{3+} .^[42] Then, the optical transmittance returned back to a quasi-plateau and the solution became transparent again as the concentration of Eu^{3+} continuously increased, because the excess amount of Eu^{3+} may interfere with the intermolecular aggregation of $(\text{Eu}^{3+}@\text{Azo-DPA})\text{-}\alpha\text{-CD}$ complex. Meanwhile, the FTIR spectrum further confirmed the successful coordination between Azo-DPA and Eu^{3+} ion; that is, compared to the individual Azo-DPA, the band at 1713 cm^{-1} assigned to C=O stretching vibration completely disappeared in the $\text{Eu}^{3+}@\text{Azo-DPA}$ complex (Figure S15, Supporting Information). These spectroscopic data substantiate the

existence of azophenyl group cannot make any negative impact on the metal–ligand coordination between Eu^{3+} and DPA and undoubtedly, the high coordination numbers and strong metal–ligand interaction would effectively sensitize Eu^{3+} and simultaneously avoid the undesired attack from water molecules.^[43]

It has been reported that most of azobenzene derivatives are non-fluorescent species, owing to their fast-conformational transition around the central N=N bond.^[28–30] As expected, in our case, the $\text{Eu}^{3+}@\text{Azo-DPA}$ solution exhibited imperceptible fluorescence emission after excitation, indicating that the incorporation of azophenyl unit into lanthanide complex seriously dissipated the energy of the excited state. In keen contrast, with the gradual addition of $\alpha\text{-CD}$ into the $\text{Eu}^{3+}@\text{Azo-DPA}$ solution, the characteristic emission of Eu^{3+} was largely enhanced with five sharp peaks at 577 nm ($^5\text{D}_0 \rightarrow ^7\text{F}_0$), 590 nm ($^5\text{D}_0 \rightarrow ^7\text{F}_1$), 613 nm ($^5\text{D}_0 \rightarrow ^7\text{F}_2$), 648 nm ($^5\text{D}_0 \rightarrow ^7\text{F}_3$) and 689 nm ($^5\text{D}_0 \rightarrow ^7\text{F}_4$) (Figure 2a). The luminescence intensity of $\text{Eu}^{3+}@\text{Azo-DPA}$ solution with $\alpha\text{-CD}$ incredibly increased nearly 50-fold at 613 nm as compared to that without $\alpha\text{-CD}$. Meanwhile, the $(\text{Eu}^{3+}@\text{Azo-DPA})\text{-}\alpha\text{-CD}$ complex exhibited bright red emission with a quantum yield of 1.7% and a lifetime of 100.8 μs , respectively (Figure S17, Supporting Information). More interestingly, after irradiated with UV light for 7 min, the luminescence intensity of $(\text{Eu}^{3+}@\text{Azo-DPA})\text{-}\alpha\text{-CD}$

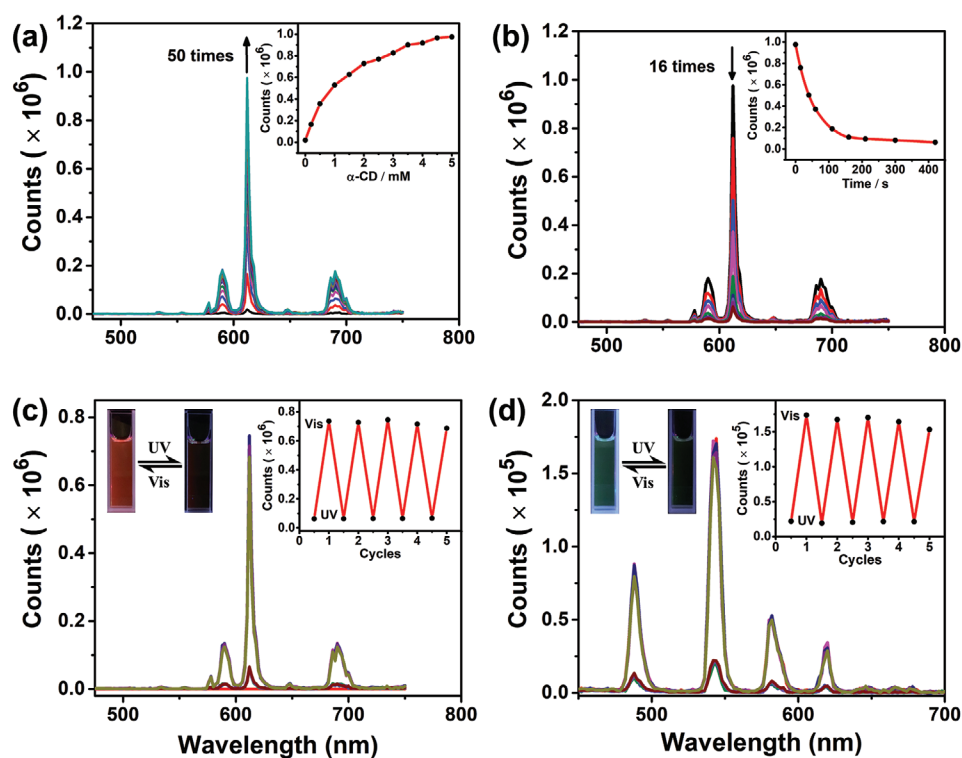


Figure 2. a) Photoluminescence spectra and emission intensity changes at 613 nm (inset) of (a) Eu^{3+} @Azo-DPA complex ($[\text{Azo-DPA}] = 0.1 \times 10^{-3}$ M, $[\text{Eu}^{3+}] = 0.067 \times 10^{-3}$ M) upon addition of α -CD ($0\text{--}5 \times 10^{-3}$ M) in aqueous solution ($\lambda_{\text{ex}} = 254$ nm); b) $(\text{Eu}^{3+}$ @Azo-DPA) \subset α -CD complex ($[\alpha\text{-CD}] = 5 \times 10^{-3}$ M) upon UV irradiation at 365 nm; c) $(\text{Eu}^{3+}$ @Azo-DPA) \subset α -CD complex upon consecutively alternating exposure to UV and visible light; d) Photoluminescence spectra and emission intensity changes at 544 nm (inset) of $(\text{Tb}^{3+}$ @Azo-DPA) \subset α -CD complex upon consecutively alternating exposure to UV and visible light ($[\text{Azo-DPA}] = 0.1 \times 10^{-3}$ M, $[\text{Tb}^{3+}] = 0.067 \times 10^{-3}$ M, $[\alpha\text{-CD}] = 5 \times 10^{-3}$ M, $\lambda_{\text{ex}} = 254$ nm).

complex was gradually quenched by 94% and the red emission was no longer observed at the photostationary state (Figure 2b). It was also noteworthy that the quenched luminescence of $(\text{Eu}^{3+}$ @Azo-DPA) \subset α -CD complex could be largely recovered upon the visible light irradiation at 450 nm for only 40 s. The photoswitchable luminescence process could be conducted for several times without noticeable light fading (Figure 2c). Similarly, such photo-controlled reversible luminescence behaviors were also observed for the $(\text{Tb}^{3+}$ @Azo-DPA) \subset α -CD complex (Figure 2d). The complexation with α -CD could result in a 15-fold enhancement of the characteristic emission at 544 nm of Tb^{3+} (Figure S18, Supporting Information). The quantum yield and lifetime were measured as 1.0% and 74.2 μs , respectively (Figure S19, Supporting Information). After exposed to UV irradiation, the luminescence intensity was quenched by 91%, and the fluorescence emission was largely recovered under visible light irradiation. In addition, control experiments demonstrated that the fluorescence emission was achieved only when Eu^{3+} @*trans*-Azo-DPA complex was encapsulated in the cavity of α -CD and the addition of α -CD had no influence on the emission intensity of Eu^{3+} @DPA complex (Figures S20 and S21, Supporting Information). These results jointly suggest that the host–guest complexation of *trans*-azobenzene moiety with α -CD is a prerequisite for achieving the photoswitchable lanthanide luminescence process. Besides, the reference compound without DPA group (Azo-im) was synthesized to investigate

the interaction between the N = N bond and lanthanide ion by NMR and UV–vis absorption spectroscopy. These experimental results suggested that no spectral change was found when Eu^{3+} was added to the Azo-im solution, thus excluding the possibility that the N=N group could participate in the coordination with lanthanide ion (Figures S22 and S23, Supporting Information). Also, 15% DMF–H₂O was introduced to the Eu^{3+} @Azo-DPA solution to avoid the self-assembled chromophore aggregation. As revealed by optical transmittance experiment results, no decline in transmittance was observed in the presence of 1/3 equiv of Eu^{3+} , implying the chromophore self-aggregation was completely eliminated in this case (Figure S24a, Supporting Information). Similarly, the photoluminescence spectra showed that the Eu^{3+} @Azo-DPA complex only showed faint emission and the luminescent intensity was significantly enhanced by 24 times upon addition of excess α -CD (Figure S24b, Supporting Information). Therefore, it is concluded that when the molecular conformation was immobilized by the host–guest complexation with α -CD in solution, and the emissive path revived to dramatically augment the luminescence efficiency.

To deep understand the photoswitchable luminescence mechanism, density functional theory (DFT) calculations were performed by means of the Gaussian 16 program. As revealed by the geometry optimization and energy calculation, when the dihedral angle of C–N=N–C (φ) was 180° in the ground state (S_0), the overall structure of Azo-DPA possessed the minimum

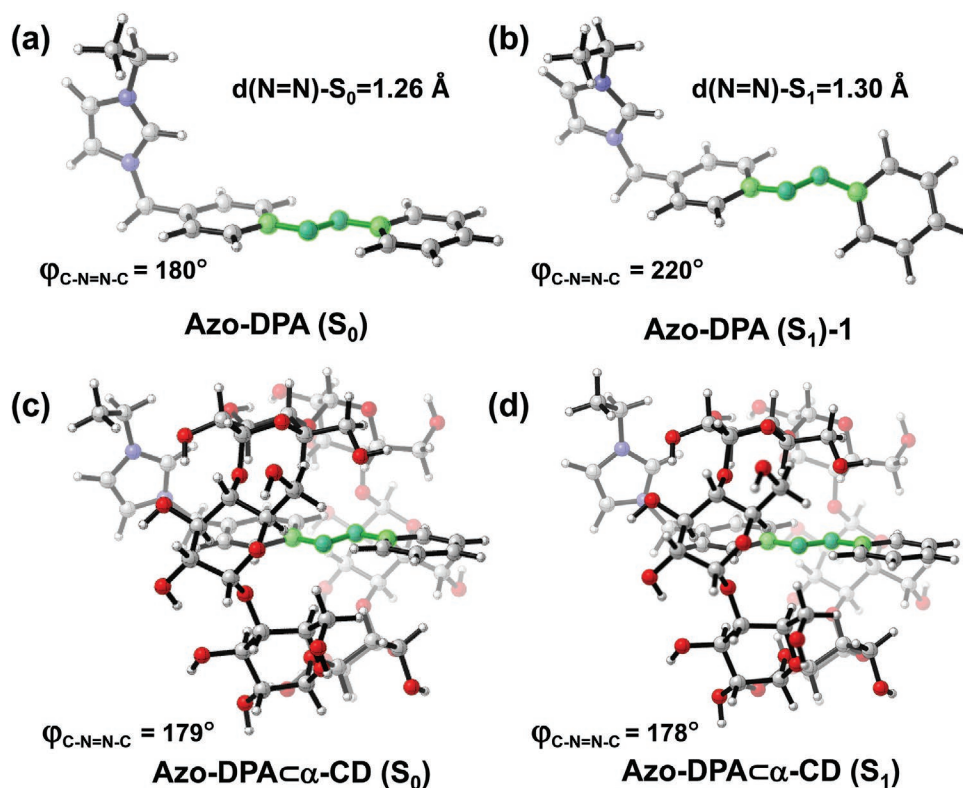


Figure 3. Optimized molecular geometries of Azo-DPA and Azo-DPA@ α -CD complex in the a,c) ground state (S_0) and b,d) singlet excited (S_1) state, respectively.

energy, which could be assigned as the most stable geometric conformation (Figure 3a and Figure S25a, Supporting Information). However, when Azo-DPA was located in the first excited singlet state (S_1), the most stable conformation was screened at the torsion angles of $\varphi = 140^\circ$ and 220° (Figure 3b). The interconversion of the two most stable isomers required the activation energies of 5.1 and 5.7 kcal/mol, respectively (Figure S25b). In addition, the $\text{N}=\text{N}$ bond was elongated from 1.26 Å in the S_0 state to 1.30 Å in the S_1 state. These results indicate the central $\text{N}=\text{N}$ bond has tendency to rotate in the S_1 state. Consequently, the nonradiative relaxation through the rotation of $\text{N}=\text{N}$ bond would dissipate the energy of the excited state and result in the fluorescence quenching. Comparatively, in the case of Azo-DPA@ α -CD inclusion complex, the dihedral angles remained almost unchanged in the both S_0 and S_1 states, implying that the host-guest inclusion with α -CD could largely stabilize the molecular conformation and inhibit the nonradiative molecular rotation in the excited state, thus enhancing the luminescence efficiency (Figure 3c,d). Moreover, the quantum calculation studies also confirmed that when the *trans*-azobenzene was converted to the geometry-optimized *cis*-isomer, its interatomic distance became larger than the inner diameter of α -CD, which could not form the stable host-guest complex (Figure S26, Supporting Information). Taken together, the confinement effect makes the encapsulated *trans*-azobenzene more immovable in the α -CD's cavity and thus the emissive path of lanthanide complex revives to dramatically augment the photoluminescence efficiency.

It is noted that *cis*-azobenzenes could undergo thermal isomerization back to the more stable *trans* isomer. Thus, the thermal *cis*-to-*trans* isomerization kinetics was studied by monitoring the spontaneous recovery of the π - π^* transition absorption at 320 nm in the photostationary state under light irradiation at 365 nm. The half-life times ($t_{1/2}$) of *cis*-Azo-DPA and *cis*-Azo-DPA/ α -CD at room temperature were estimated to be 15.1 and 14.9 days, respectively. In comparison, this $t_{1/2}$ value decreased to 6.7 days after coordination with Eu^{3+} (Figure S27, Supporting Information). These results demonstrate that the *cis*-to-*trans* photoisomerization can be greatly accelerated especially in the presence of lanthanide ion and thus facilitate the fluorescence recovery of supramolecular lanthanide photoswitch.

Hydrogels are considered as an ideal type of nanomaterials for stretchable display and information storage. With the processable CD-confined lanthanide complex in hand, the supramolecularly cross-linked hydrogels could be conveniently obtained via free-radical copolymerization in the presence of the acrylamide-modified α -CD (AAm- α -CD) and Eu^{3+} @Azo-DPA complex. Scanning electron microscopic (SEM) images showed that the morphology of porous networks was retained before and after UV light irradiation (Figure 4a and Figure S28, Supporting Information). Meanwhile, the strain sweep test in the rheological experiments revealed that the storage modulus G' was always larger than the loss modulus G'' even when the oscillating strain reached up to 400% (Figure S29a, Supporting Information). When the strain was fixed at 1%, the frequency

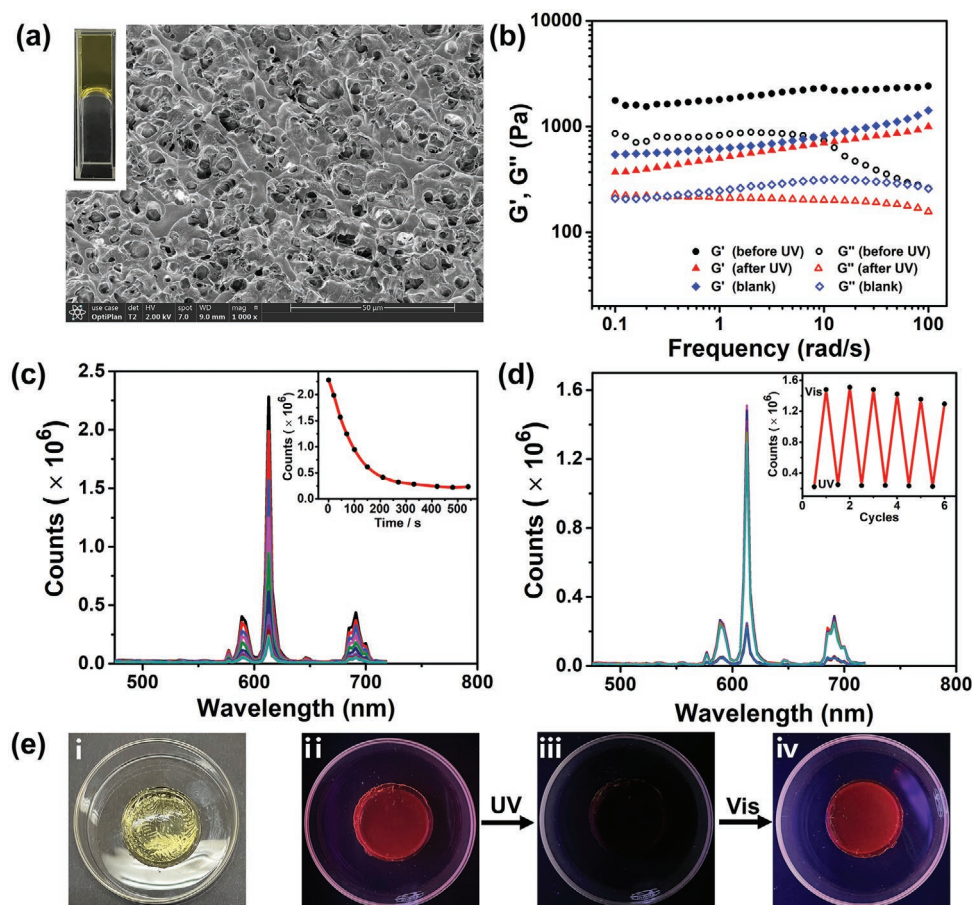


Figure 4. a) SEM images and photograph (inset) of supramolecular hydrogels. b) Frequency sweep tests at $\omega = 0.1\text{--}100\text{ rad s}^{-1}$ and strain (γ) = 1.0% for the control hydrogels (blue squares) and Eu^{3+} -containing hydrogels before (black circles) and after (red triangles) UV irradiation. c) Photoluminescence spectra and emission intensity changes at 613 nm (inset) of Eu^{3+} -containing hydrogels upon c) irradiation with UV light irradiation at 365 nm and d) consecutively alternating exposure to UV (365 nm, 7 min) and visible light (450 nm, 40 s). e) Photographs of the supramolecular hydrogel i) under daylight and ii–iv) upon alternating UV and visible light irradiation. The control hydrogel was prepared by polymerization of acrylamide without ($\text{Eu}^{3+}@Azo\text{-DPA}$) $\text{-}\alpha\text{-CD}$ complex.

sweep tests showed that G' remained larger than G'' in the applied frequency range, indicative of the formation of quite stable hydrogel (Figure 4b). Benefiting from the cross-linking by host–guest interactions and synergistic metal–coordination interactions, this was also found that the incorporation of supramolecular complexes could markedly enhance the mechanical strength of the hydrogel. Although both G' and G'' values of the as-prepared hydrogel were declined to some extent after UV light irradiation, G' still maintained a higher value than G'' and no phase transition occurred during light irradiation (Figure S29b, Supporting Information). Upon excitation, the obtained hydrogel emitted bright red fluorescence, corresponding to the characteristic emission of ($\text{Eu}^{3+}@Azo\text{-DPA}$) $\text{-}\alpha\text{-CD}$ complex. The quantum yield and lifetime of such multicomponent hydrogel were obtained as 2.5% and 155.6 μs , respectively (Figure S30 and Table S1, Supporting Information). In line with the phenomena observed in aqueous solution, the hydrogel also exhibited photoswitchable luminescence behaviors with excellent fatigue resistance. The emission intensity at 613 nm was quenched by 90% when irradiated with UV light, and then recovered to the original level under the subsequent visible light

irradiation (Figure 4c,d). In addition, the photoluminescence of obtained hydrogel could be intuitively recognized and concealed upon alternative exposure to UV and visible light irradiation (Figure 4e).

3. Conclusion

In conclusion, we have successfully constructed a photo-switchable luminescent supramolecular system using $\alpha\text{-CD}$ and the azobenzene-modified lanthanide complex both in aqueous solution and gel state. As investigated by the spectroscopic experiments and computational studies, the photoisomerization property of azobenzene could be completely reserved and the nonradiative energy loss of azobenzene could be efficiently reduced by the tight host–guest complexation, thereby leading to the activation of the inherent emission of lanthanide complex. More significantly, through the photoisomeric association and disassociation between $\alpha\text{-CD}$ and azobenzene, the photoluminescence of supramolecular lanthanide complexes could be reversibly regulated by irradiating at different wavelengths. To

be envisaged, extending our strategy can make the macrocycle-confined photoisomeric lanthanide complex an appealing candidate in the creation of light-responsive intelligent materials.

Supporting Information

Supporting Information is available from the Wiley Online Library or from the author.

Acknowledgements

This work was financially supported by the National Natural Science Foundation of China (grants 21871154, 22171148, 22131008, 21873051, 21801135), Natural Science Foundation of Tianjin (21JCZDJC00310), the Fundamental Research Funds for the Central Universities (Nankai University) and the Haihe Laboratory of Sustainable Chemical Transformations.

Conflict of Interest

The authors declare no conflict of interest.

Data Availability Statement

The data that support the findings of this study are available in the supplementary material of this article.

Keywords

azobenzene, conformational confinement, cyclodextrin, lanthanide complexes, switchable luminescence

Received: March 19, 2022

Revised: April 10, 2022

Published online:

- [1] R. Zhang, J. Yuan, *Acc. Chem. Res.* **2020**, *53*, 1316.
 [2] W. Guan, W. Zhou, J. Lu, C. Lu, *Chem. Soc. Rev.* **2015**, *44*, 6981.
 [3] J. Chen, L. Chen, Y. Wu, Y. Fang, F. Zeng, S. Wu, Y. Zhao, *Nat. Commun.* **2021**, *12*, 6870.
 [4] H.-J. Yu, Q. Zhou, X. Dai, F.-F. Shen, Y.-M. Zhang, X. Xu, Y. Liu, *J. Am. Chem. Soc.* **2021**, *143*, 13887.
 [5] J. Zhang, B. He, Y. Hu, P. Alam, H. Zhang, J. W. Y. Lam, B. Z. Tang, *Adv. Mater.* **2021**, *33*, 2008071.
 [6] L. Ding, X.-d. Wang, *J. Am. Chem. Soc.* **2020**, *142*, 13558.
 [7] H. Zhang, Q. Li, Y. Yang, X. Ji, J. L. Sessler, *J. Am. Chem. Soc.* **2021**, *143*, 18635.
 [8] H. Kaur, S. Sundriyal, V. Pachauri, S. Ingebrandt, K.-H. Kim, A. L. Sharma, A. Deep, *Coord. Chem. Rev.* **2019**, *401*, 213077.
 [9] Y. Tian, J. Yang, Z. Liu, M. Gao, X. Li, W. Che, M. Fang, Z. Li, *Angew. Chem., Int. Ed.* **2021**, *60*, 20259.
 [10] Z. Zhou, M. Vázquez-González, I. Willner, *Chem. Soc. Rev.* **2021**, *50*, 4541.
 [11] Y.-M. Zhang, Y.-H. Liu, Y. Liu, *Adv. Mater.* **2020**, *32*, 1806158.
 [12] T. L. Mako, J. M. Racicot, M. Levine, *Chem. Rev.* **2019**, *119*, 322.
 [13] X.-Y. Lou, Y.-W. Yang, *Adv. Mater.* **2020**, *32*, 2003263.
 [14] H. Wu, Y. Chen, X. Dai, P. Li, J. F. Stoddart, Y. Liu, *J. Am. Chem. Soc.* **2019**, *141*, 6583.
 [15] Y. Zhou, H.-Y. Zhang, Z.-Y. Zhang, Y. Liu, *J. Am. Chem. Soc.* **2017**, *139*, 7168.
 [16] J. Kim, H. Yun, Y. J. Lee, J. Lee, S.-H. Kim, K. H. Ku, B. J. Kim, *J. Am. Chem. Soc.* **2021**, *143*, 13333.
 [17] M. Dong, A. Babalhavaeji, S. Samanta, A. A. Beharry, G. A. Woolley, *Acc. Chem. Res.* **2015**, *48*, 2662.
 [18] L. Dong, Y. Feng, L. Wang, W. Feng, *Chem. Soc. Rev.* **2018**, *47*, 7339.
 [19] C. Probst, C. Meichner, K. Kreger, L. Kador, C. Neuber, H.-W. Schmidt, *Adv. Mater.* **2016**, *28*, 2624.
 [20] Y.-H. Liu, Y. Liu, *Prog. Chem.* **2019**, *31*, 1528.
 [21] G. Yu, C. Han, Z. Zhang, J. Chen, X. Yan, B. Zheng, S. Liu, F. Huang, *J. Am. Chem. Soc.* **2012**, *134*, 8711.
 [22] J. Yao, W. Wu, C. Xiao, D. Su, Z. Zhong, T. Mori, C. Yang, *Nat. Commun.* **2021**, *12*, 2600.
 [23] C. Gao, Q. Huang, Q. Lan, Y. Feng, F. Tang, M. P. M. Hoi, J. Zhang, S. M. Y. Lee, R. Wang, *Nat. Commun.* **2018**, *9*, 2967.
 [24] Y. Liu, T. Pan, Y. Fang, N. Ma, S. Qiao, L. Zhao, R. Wang, T. Wang, X. Li, X. Jiang, F. Shen, Q. Luo, J. Liu, *ACS Catal.* **2017**, *7*, 6979.
 [25] L. Stricker, E.-C. Fritz, M. Peterlechner, N. L. Doltsinis, B. J. Ravoo, *J. Am. Chem. Soc.* **2016**, *138*, 4547.
 [26] Y.-M. Zhang, N.-Y. Zhang, K. Xiao, Q. Yu, Y. Liu, *Angew. Chem., Int. Ed.* **2018**, *57*, 8649.
 [27] M. Zhao, B. Li, P. Wang, L. Lu, Z. Zhang, L. Liu, S. Wang, D. Li, R. Wang, F. Zhang, *Adv. Mater.* **2018**, *30*, 1804982.
 [28] H. M. D. Bandara, S. C. Burdette, *Chem. Soc. Rev.* **2012**, *41*, 1809.
 [29] I. K. Lednev, T.-Q. Ye, P. Matousek, M. Towrie, P. Fogg, F. V. R. Neuwahl, S. Umapathy, R. E. Hester, J. N. Moore, *Chem. Phys. Lett.* **1998**, *290*, 68.
 [30] M. Poprawa-Smoluch, J. Baggerman, H. Zhang, H. P. A. Maas, L. De Cola, A. M. Brouwer, *J. Phys. Chem. A* **2006**, *110*, 11926.
 [31] W. Piao, S. Tsuda, Y. Tanaka, S. Maeda, F. Liu, S. Takahashi, Y. Kushida, T. Komatsu, T. Ueno, T. Terai, T. Nakazawa, M. Uchiyama, K. Morokuma, T. Nagano, K. Hanaoka, *Angew. Chem., Int. Ed.* **2013**, *52*, 13028.
 [32] J. Yoshino, N. Kano, T. Kawashima, *Chem. Commun.* **2007**, 559.
 [33] M. Gon, K. Tanaka, Y. Chujo, *Angew. Chem., Int. Ed.* **2018**, *57*, 6546.
 [34] Q. Zhu, S. Wang, P. Chen, *Org. Lett.* **2019**, *21*, 4025.
 [35] G. Ouyang, D. Bialas, F. Würthner, *Org. Chem. Front.* **2021**, *8*, 1424.
 [36] D.-H. Qu, F.-Y. Ji, Q.-C. Wang, H. Tian, *Adv. Mater.* **2006**, *18*, 2035.
 [37] D.-H. Qu, Q.-C. Wang, H. Tian, *Angew. Chem., Int. Ed.* **2005**, *44*, 5296.
 [38] J.-C. G. Bünzli, C. Piguet, *Chem. Rev.* **2002**, *102*, 1897.
 [39] W.-L. Zhou, Y. Chen, Y. Liu, *Acta Chim. Sinica.* **2020**, *78*, 1164.
 [40] W.-L. Zhou, Y. Chen, W. Lin, Y. Liu, *Chem. Commun.* **2021**, *57*, 11443.
 [41] Z. Li, G. Wang, Y. Wang, H. Li, *Angew. Chem., Int. Ed.* **2018**, *57*, 2194.
 [42] L. Xu, L. Feng, Y. Han, Y. Jing, Z. Xian, Z. Liu, J. Huang, Y. Yan, *Soft Matter* **2014**, *10*, 4686.
 [43] M. R. George, C. A. Golden, M. C. Grossel, R. J. Curry, *Inorg. Chem.* **2006**, *45*, 1739.